

Search for electromagnetic properties of the neutrino in γe and $\gamma\gamma$ collisions at CLIC

A. Senol*

Department of Physics, Kastamonu University, 37100, Kastamonu, Turkey

Abstract

We have examined nonstandard $\gamma\nu\bar{\nu}$ and $\gamma\gamma\nu\bar{\nu}$ couplings via $\nu\bar{\nu}$ production in a $e\gamma$ and $\gamma\gamma$ collisions at the CLIC. We obtain 95 % confidence level bounds on $\gamma\nu\bar{\nu}$ and $\gamma\gamma\nu\bar{\nu}$ couplings by considering the backscattered photon distribution function for incoming photons and Initial State Radiation (ISR) and Beamstrahlung (BS) effect for initial state electrons in the $e\gamma$ and $\gamma\gamma$ collider modes of linear collider. We indicate that the reaction $\gamma\gamma \rightarrow \nu\bar{\nu}$ provides more than 15 orders of magnitude improvement in neutrino-two photon couplings compared to LEP limits.

PACS numbers: 13.15.+g, 12.60.-i, 14.60.St

*Electronic address: asenol@kastamonu.edu.tr

I. INTRODUCTION

Searches on electromagnetic properties of neutrinos have become one of the important issue in particle physics, astrophysics and cosmology after observation of neutrino oscillations gives evidence that the neutrino mass is non-zero [1–3]. Moreover, this searching may play a key role to understanding the physics beyond the Standard Model (SM) and contributes to studies in astrophysics and cosmology. Although, the coupling of neutrino-photon ($\nu\bar{\nu}\gamma$) and neutrino two-photon ($\nu\bar{\nu}\gamma\gamma$) interactions by evaluating radiative diagrams in the simplest extension of SM with massive neutrinos are very small, there are several models beyond SM, predicting relatively large coupling. Thus, one of the best method to research electromagnetic properties of neutrinos is a model-independent way.

Anomalous properties of neutrinos will already be well known from The CERN Large Hadron Collider (LHC) data before a TeV scale linear collider runs, since the LHC can produce very massive new particles and will extend the possibilities of testing for new physics effects. Nevertheless, the LHC may not provide precision measurements as a result of the typical characteristic of hadron machine. Whereas, a linear collider with energies on the TeV scale, extremely high luminosity and clean experimental environment, can provide complementary information for these properties with performing precision measurements that would complete the LHC results. A most popular proposed linear colliders with energies on the TeV scale ($\sqrt{s} = 3$ TeV) and extremely high luminosity (10^{35} cm $^{-2}$ s $^{-1}$) is Compact Linear Collider (CLIC) [4]. CLIC generates an accelerating gradient of 150 MVm $^{-1}$ with the resulting 20 km of active length. CLIC uses two beam accelerator technology operating at 30 GHz radio frequency to reach this high accelerating gradient. In addition to e^+e^- , linear colliders provide a suitable platform to study $\gamma\gamma$ and γe interactions at energies and luminosities comparable to those e^+e^- collisions through the laser backscattering procedure [5, 6].

The most sensitive experimental bounds on neutrino magnetic moment are obtained from neutrino-electron scattering experiment with reactor neutrinos [7–10] and solar neutrinos [11], where these limits are about order of $10^{-11}\mu_B$. Another bounds on magnetic moment of neutrinos derived from energy loss of astrophysical objects give about an order of magnitude more restrictive constraint than reactor and solar neutrino probes [12–18].

Although, $\gamma\nu\bar{\nu}$ coupling attract too much attention, $\gamma\gamma\nu\bar{\nu}$ coupling has been much less

studied in literature. Current experimental bound on $\gamma\gamma\nu\bar{\nu}$ coupling was obtained from the LEP data via $Z \rightarrow \nu\bar{\nu}\gamma\gamma$ decay as follows [19]:

$$\left[\frac{1\text{GeV}}{\Lambda}\right]^6 \sum_{i,j,k} (|\alpha_{Rk}^{ij}|^2 + |\alpha_{Lk}^{ij}|^2) \leq 2.85 \times 10^{-9} \quad (1)$$

and the analysis of Primakoff effect on $\nu_\mu N \rightarrow \nu_s N$ conversion in the external Coulomb field of the nucleus N yields about two orders of magnitude more restrictive bound than $Z \rightarrow \nu\bar{\nu}\gamma\gamma$ decay. In refs. [21, 22], the potential of γp and $\gamma\gamma$ collision at the LHC was studied to probe neutrino-photon and neutrino-two photon coupling. In [21] was shown that the reaction $pp \rightarrow p\gamma p \rightarrow p\nu\bar{\nu}qX$ provides more than eight orders of magnitude improvement in $\gamma\gamma\nu\bar{\nu}$ couplings compared to LEP limits.

The purpose of the present paper is to report on the possibility of obtaining indirect bounds on electromagnetic properties of neutrinos from anomalous $\gamma\nu\bar{\nu}$ and $\gamma\gamma\nu\bar{\nu}$ couplings via $e^-\gamma \rightarrow \nu\bar{\nu}e^-$ and $\gamma\gamma \rightarrow \nu\bar{\nu}$ processes at the CLIC.

II. EFFECTIVE LAGRANGIAN FOR $\gamma\nu\bar{\nu}$ AND $\gamma\gamma\nu\bar{\nu}$ INTERACTIONS

The magnetic moment couple neutrinos to photon through the dimension-6 effective Lagrangian term

$$\mathcal{L} = \frac{1}{2}\mu_{ij}\bar{\nu}_i\sigma_{\mu\nu}\nu_j F^{\mu\nu} \quad (2)$$

where $F^{\mu\nu}$ is the electromagnetic field tensor, i, j are the flavor indices, μ_{ii} is the magnetic moment of ν_i and μ_{ij} ($i \neq j$) is the transition magnetic moment. The new physics energy scale Λ is embedded in the definition of μ_{ij} in the above dimension-6 effective Lagrangian.

Now we turn to the neutrino-two-photon ($\gamma\gamma\nu\bar{\nu}$) vertex which describing from following dimension-7 effective Lagrangian:

$$\mathcal{L} = \frac{1}{4\Lambda^3}\bar{\nu}_i (\alpha_{R1}^{ij}P_R + \alpha_{L1}^{ij}P_L) \nu_j \tilde{F}_{\mu\nu} F^{\mu\nu} + \frac{1}{4\Lambda^3}\bar{\nu}_i (\alpha_{R2}^{ij}P_R + \alpha_{L2}^{ij}P_L) \nu_j F_{\mu\nu} F^{\mu\nu} \quad (3)$$

where $P_{L(R)} = \frac{1}{2}(1 \mp \gamma_5)$, $\tilde{F}_{\mu\nu} = \frac{1}{2}\epsilon_{\mu\nu\alpha\beta}F^{\alpha\beta}$, α_{Lk}^{ij} and α_{Rk}^{ij} are dimensionless coupling constants. We will focus on Dirac neutrino case and obtain model independent bounds on couplings using effective Lagrangians (2) and (3).

In this study we consider $e^-\gamma \rightarrow \nu\bar{\nu}e^-$ and $\gamma\gamma \rightarrow \nu\bar{\nu}$ processes for searching non-standard $\nu\bar{\nu}\gamma$ and $\gamma\gamma\nu\bar{\nu}$ interactions which denotes Lagrangians (2) and (3). The complete sets of

Feynman diagrams contributing to $e^-\gamma \rightarrow \nu\bar{\nu}e^-$ at tree level are shown in Figs. 1 and 2. As seen from Fig.1, the first six diagrams((a)-(f)) contains nonstandard $\nu\bar{\nu}\gamma$ vertices and the last two diagrams ((g) and (h)) comes from SM electroweak processes.

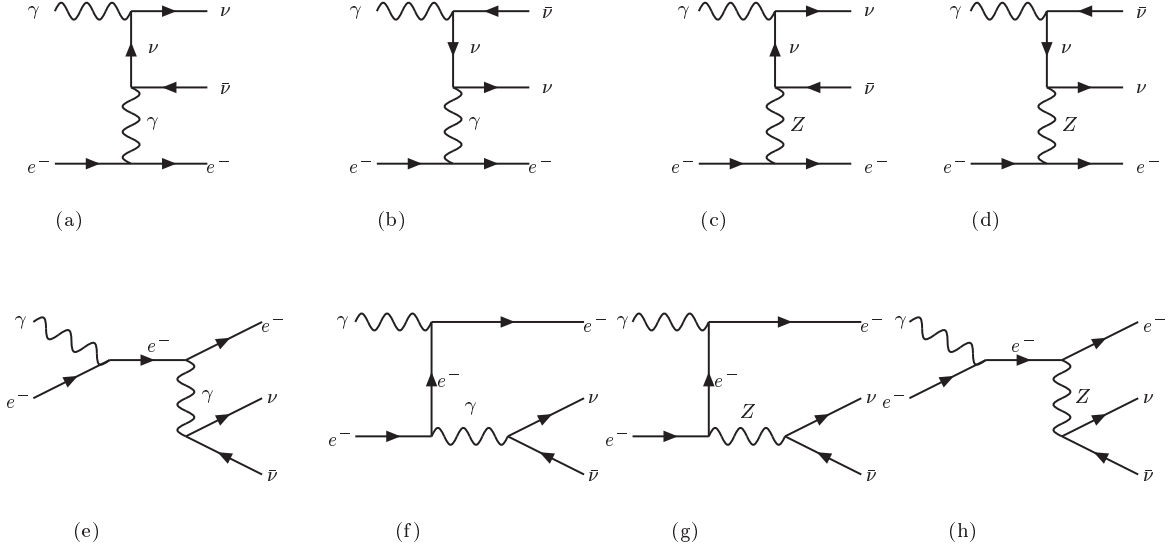


FIG. 1: Tree-level Feynman diagrams for the process $e^-\gamma \rightarrow \nu\bar{\nu}e^-$ in the existence of non-standard $\nu\bar{\nu}\gamma$ coupling.

As shown in Fig.2, we have only three Feynman diagrams in the presence of the effective interaction (3). Fig. 3 shows the Feynman diagrams of $\gamma\gamma \rightarrow \nu\bar{\nu}$ process which consists of only non-standard $\nu\bar{\nu}\gamma$ and $\gamma\gamma\nu\bar{\nu}$ interaction vertices. In order to examine all numerical calculations, we have implemented the $\gamma\nu\bar{\nu}$ and $\gamma\gamma\nu\bar{\nu}$ vertices into the tree-level event generator CompHEP [20]. In this study, we consider Initial State Radiation (ISR) for incoming electron. ISR is a process of photon radiation by the incoming electron due to its interaction with other collision particle. In addition to this, we take into account this spectrum in our calculations by using the CompHEP program with beamstrahlung spectra. Beamstrahlung is a process of energy loss by the incoming electron due to its interaction with the positron (electron) bunch moving in the opposite direction. Beamstrahlung spectrum, which depends on the bunch geometry, bunch charge and the collision energy, is an attribute of the linear collider design. When calculating these effects we take into account the beam parameters of the CLIC as shown in Table I

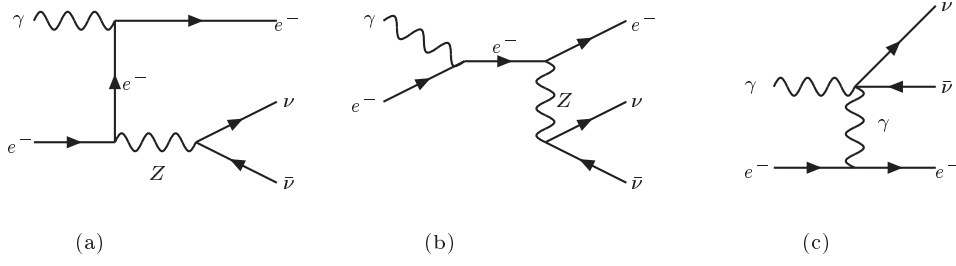


FIG. 2: Tree-level Feynman diagrams for the subprocess $e^-\gamma \rightarrow \nu\bar{\nu}e^-$ in the existence of non-standard $\nu\bar{\nu}\gamma\gamma$ coupling.

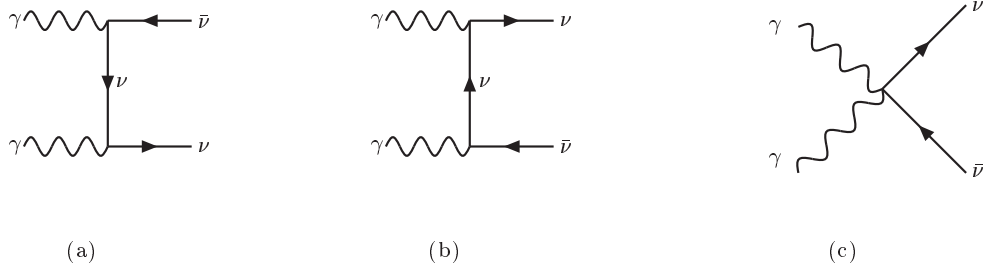


FIG. 3: Tree-level Feynman diagrams for the subprocess $\gamma\gamma \rightarrow \nu\bar{\nu}$ in the existence of non-standard both $\nu\bar{\nu}\gamma$ and $\nu\bar{\nu}\gamma\gamma$ couplings.

TABLE I: The beam parameters of the two energy options of the CLIC. N is the number of particles in the electron bunch, $\sigma_{x,y,z}$ are the average sizes of the electron bunches and \mathcal{L} is the design luminosity.

parameter	$\sqrt{s}=0.5$ TeV	$\sqrt{s}=3$ TeV
$\mathcal{L}(\text{cm}^{-2}\text{s}^{-1})$	$2.3 \cdot 10^{34}$	$5.9 \cdot 10^{34}$
$N(10^9)$	6.8	3.72
$\sigma_x(\text{nm})$	200	45
$\sigma_y(\text{nm})$	2.3	1
$\sigma_z(\mu\text{m})$	72	44

Now, we will analyze the $\nu\bar{\nu}\gamma$ coupling on the process $e^-\gamma \rightarrow \nu\bar{\nu}e^-$ assuming neutrino magnetic moment matrix is almost flavor diagonal ($\mu_{\nu_i} \gg \mu_{\nu_i\nu_j}$) and only one of the matrix elements is different from zero ($\mu_{\nu_i} = \mu$). In Figs.4 and 5, we plot the total cross sections for $e^-\gamma \rightarrow \nu\bar{\nu}e^-$ as a function of anomalous coupling μ with and without ISR and beamstrahlung effects for center of mass energies 3 TeV and 0.5 TeV, respectively.

Fig.2 shows the total cross sections of $e^-\gamma \rightarrow \nu\bar{\nu}e^-$ process depending on anomalous part as function of $\alpha_1^2 + \alpha_2^2$ are calculated in the case of effective interaction (3). Here, α_1 and α_2 can written in the form:

$$\alpha_1^2 = \sum_{i,j} [|\alpha_{R1}^{ij}|^2 + |\alpha_{L1}^{ij}|^2], \quad \alpha_2^2 = \sum_{i,j} [|\alpha_{R2}^{ij}|^2 + |\alpha_{L2}^{ij}|^2] \quad (4)$$

The total cross sections for $e^-\gamma \rightarrow \nu\bar{\nu}e^-$ as a function of anomalous coupling α_1 are plotted with and without ISR and beamstrahlung effects in Fig.6 at $\sqrt{s}=3$ TeV and in Fig.7 at $\sqrt{s}=0.5$ TeV.

We have calculated analytical expression for the polarization summed amplitude square for $\gamma\gamma \rightarrow \nu\bar{\nu}$ process with CompHEP which agrees with reference [22]. Although the squared amplitude of the process depends on the anomalous couplings both α_1, α_2 and μ , we present the total cross sections of $\gamma\gamma \rightarrow \nu\bar{\nu}$ as functions of α_1 and μ in Figs. 8 for $\sqrt{s}=3$ TeV and 9 for $\sqrt{s}=0.5$ TeV at CLIC because of the fact that the dependence of cross section on α_1 and α_2 is the same.

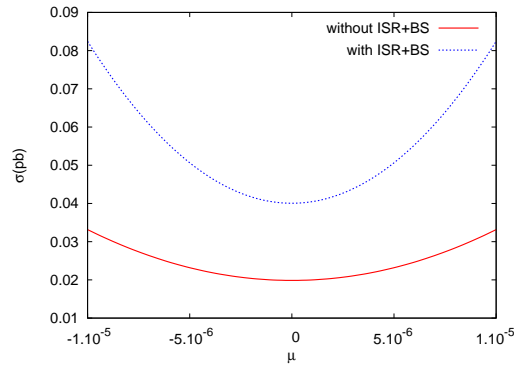


FIG. 4: The total cross section of the process $e^-\gamma \rightarrow \nu\bar{\nu}e^-$ as a function of anomalous coupling μ for the center-of-mass energy is taken to be $\sqrt{s} = 3$ TeV with and without ISR+BS effect.

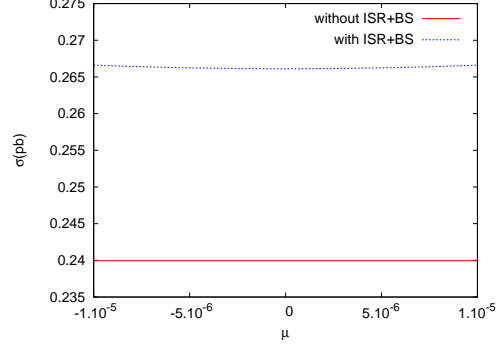


FIG. 5: The same as Fig. 4 but for $\sqrt{s}=0.5$ TeV.

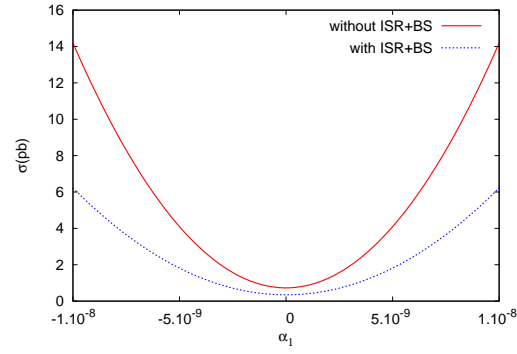


FIG. 6: The total cross section of the process $e^-\gamma \rightarrow \nu\bar{\nu}e^-$ as a function of anomalous coupling α_1 for the center-of-mass energy is taken to be $\sqrt{s} = 3$ TeV with and without ISR+BS effect.

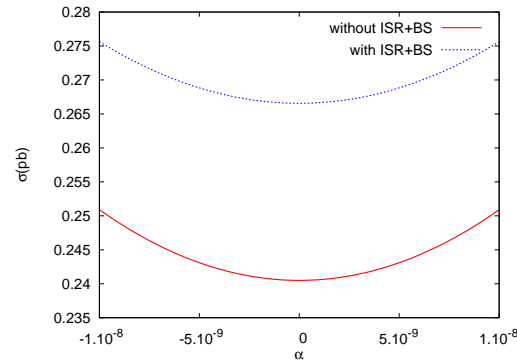


FIG. 7: The same as Fig. 6 but for $\sqrt{s}=0.5$ TeV.

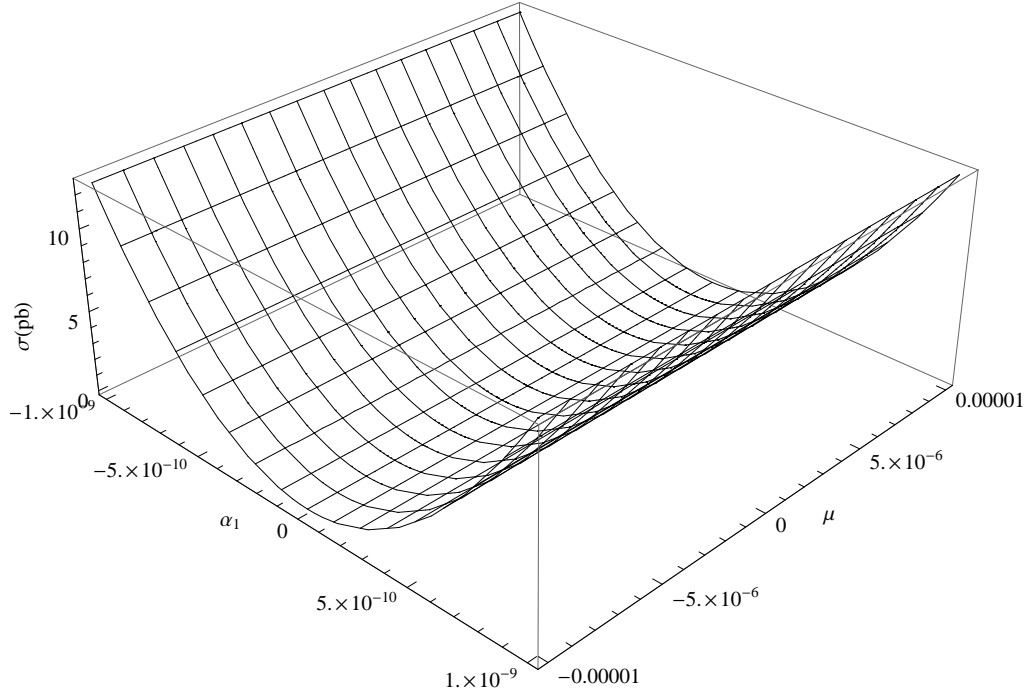


FIG. 8: The total cross section of the process $\gamma\gamma \rightarrow \nu\bar{\nu}$ as a function of anomalous couplings μ and α_1 for the center-of-mass energy is taken to be $\sqrt{s} = 3$ TeV.

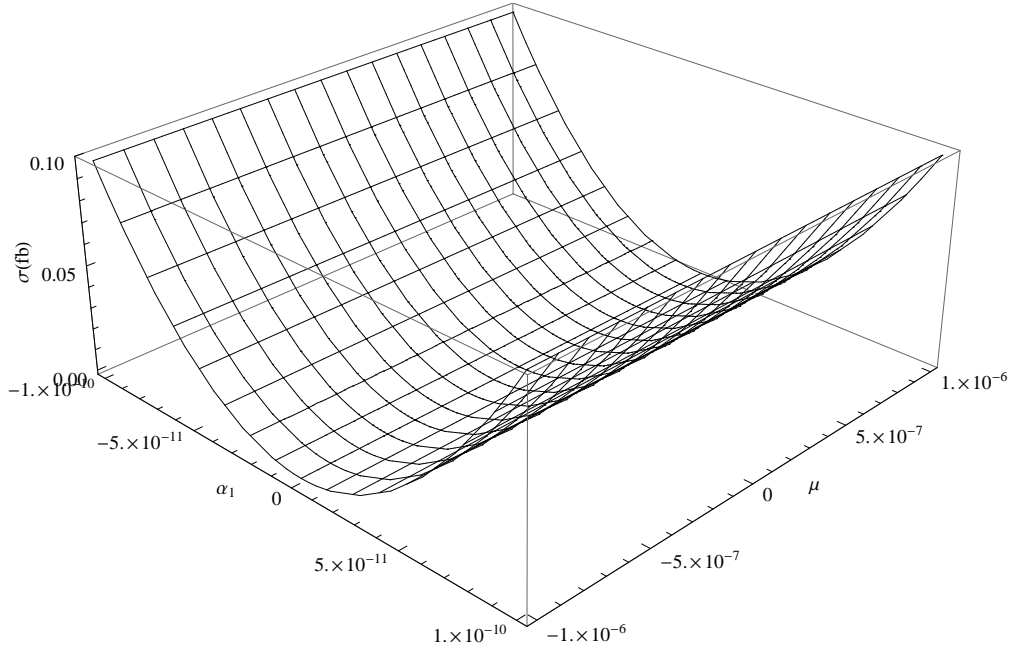


FIG. 9: The same as Fig. 8 but for $\sqrt{s}=0.5$ TeV.

III. NUMERICAL RESULTS

One-parameter χ^2 test was applied without a systematic error to obtain 95% confidence level (C.L.) on the upper limits of the α and μ . The χ^2 function is

$$\chi^2 = \left(\frac{\sigma_{SM} - \sigma_{AN}}{\sigma_{SM} \delta} \right)^2 \quad (5)$$

where σ_{AN} is the cross section containing new physics effects and $\delta = \frac{1}{\sqrt{N}}$ is the statistical error. The number of events are given by $N = \sigma_{SM} L_{int}$ where L_{int} is the integrated luminosity.

As aforementioned the neutrino magnetic moment matrix is almost flavor diagonal, because the other elements in the matrix are strictly constrained by the experiments. As well as, the element $\mu_{\tau\tau}$ is dominant over the other diagonal elements bounded with $3.9 \times 10^{-7} \mu_B$ [23]. This bound is at least 3 orders of magnitude weaker than the bounds on other diagonal matrix elements [24]. Therefore, we focus on $\mu_{\tau\tau}$ element of neutrino magnetic moment matrix in our numerical calculations. In Tables II and III, we present 95 % C.L. upper bounds of the couplings $\mu_{\tau\tau}$, α_1^2 and α_2^2 for two different center of mass energies $\sqrt{s}=3$ TeV and $\sqrt{s}=0.5$ TeV, respectively. When calculating the sensitivity of the anomalous couplings, we take into account ISR+BS effect for incoming electron and the backscattered photon distribution function for incoming photon, and also a cut of $|\eta| < 2.5$ for pseudo-rapidity of final electron for the process $e^- \gamma \rightarrow \nu \bar{\nu} e^-$. According to these tables, our limits on $\mu_{\tau\tau}$ are the same order with refs. [21, 22] but 5 times weaker than DONUT bound [23]. Besides, our limits on α_1^2 and α_2^2 ranged from order of 10^{-17} to 10^{-21} at $\sqrt{s}=0.5$ and 3 TeV for $e^- \gamma \rightarrow \nu \bar{\nu} e^-$ process as seen from Tables II and III. Our best limits on α_1^2 and α_2^2 are 10 orders of magnitude more restrictive than the LEP bound. On the other hand it is 3 orders of magnitude more restrictive than LHC bounds [21, 22].

We used a Poisson distribution for searching sensitivity to anomalous couplings through $\gamma\gamma \rightarrow \nu\bar{\nu}$ process. Because, this process is absent in the SM at tree-level. In Figs.10 and 11, we present the sensitivity contour plot at % 95 C.L. for the anomalous couplings, α_1 and μ , through $\gamma\gamma \rightarrow \nu\bar{\nu}$ process with design luminosities for $\sqrt{s}=3$ and 0.5 TeV, respectively. In addition, we show 95 % C.L. upper bounds of the couplings $\mu_{\tau\tau}$, α_1^2 and α_2^2 in Tables IV and V for two different center of mass energies $\sqrt{s}=3$ TeV and $\sqrt{s}=0.5$ TeV, respectively. As you can seen from these tables, our best limits on α_1^2 and α_2^2 are about at order of 10^{-25} , but $\mu_{\tau\tau}$ limits are one order of magnitude worse than the experimental current limits. As

TABLE II: 95% C.L. upper bounds of the couplings $\mu_{\tau\tau}$, α_1^2 and α_2^2 for the process $e^-\gamma \rightarrow \nu\bar{\nu}e^-$. We consider various values of the integrated CLIC luminosities for $\sqrt{s}=3$ TeV. Limits of $\mu_{\tau\tau}$ is given in units of Bohr magneton and Λ is taken to be 1 GeV for limits of α_1^2 and α_2^2 .

Luminosity:	$10fb^{-1}$	$30fb^{-1}$	$50fb^{-1}$	$100fb^{-1}$	$590fb^{-1}$
$\mu_{\tau\tau}$	2.68×10^{-6}	2.04×10^{-6}	1.79×10^{-6}	1.51×10^{-6}	9.67×10^{-7}
α_1^2	5.14×10^{-20}	2.97×10^{-20}	2.30×10^{-20}	1.63×10^{-20}	6.70×10^{-21}
α_2^2	5.14×10^{-20}	2.97×10^{-20}	2.30×10^{-20}	1.63×10^{-20}	6.70×10^{-21}

TABLE III: The same as table II but for $\sqrt{s}=0.5$ TeV.

Luminosity:	$10fb^{-1}$	$30fb^{-1}$	$50fb^{-1}$	$100fb^{-1}$	$230fb^{-1}$
$\mu_{\tau\tau}$	4.04×10^{-5}	3.07×10^{-5}	2.70×10^{-5}	2.27×10^{-5}	1.84×10^{-5}
α_1^2	8.89×10^{-17}	5.14×10^{-17}	3.98×10^{-17}	2.81×10^{-17}	1.85×10^{-17}
α_2^2	8.89×10^{-17}	5.14×10^{-17}	3.98×10^{-17}	2.81×10^{-17}	1.85×10^{-17}

well as our limits on α_1^2 and α_2^2 can be reached 10^{-21} at $10 fb^{-1}$ with center of mass energy of 0.5 TeV while these limits are about at the order of 10^{-19} at LHC ($\sqrt{s}=14$ TeV) with $200 fb^{-1}$ luminosity in Ref [21]. And also, these limits are 15 orders of magnitude more restrictive than LEP bound.

IV. CONCLUSIONS

We have examined the potential of $e^-\gamma \rightarrow \nu\bar{\nu}e^-$ and $\gamma\gamma \rightarrow \nu\bar{\nu}$ processes at the CLIC to search neutrino-photon and neutrino-two photon couplings. The $e\gamma$ and $\gamma\gamma$ collider modes of a linear collider probes neutrino-photon and neutrino-two photon couplings with better sensitivity than the present colliders. We have shown that the neutrino-two photon couplings improves the sensitivity limits by up to a factor of 10^{15} with respect to LEP limits. Our limits are also eight order of magnitude better than the $\nu\bar{\nu}$ production in a γp collision at the LHC [21]. Besides, neutrino-photon coupling $\mu_{\tau\tau}$ are about an order of magnitude worse than current experimental bound.

TABLE IV: 95% C.L. upper bounds of the couplings $\mu_{\tau\tau}$, α_1^2 and α_2^2 for the process $\gamma\gamma \rightarrow \nu\bar{\nu}$. We consider various values of the integrated CLIC luminosities for $\sqrt{s}=3$ TeV. Limits of $\mu_{\tau\tau}$ is given in units of Bohr magneton and Λ is taken to be 1 GeV for limits of α_1^2 and α_2^2 .

Luminosity:	$10fb^{-1}$	$30fb^{-1}$	$50fb^{-1}$	$100fb^{-1}$	$590fb^{-1}$
$\mu_{\tau\tau}$	7.37×10^{-5}	5.60×10^{-5}	4.93×10^{-5}	4.15×10^{-5}	2.67×10^{-5}
α_1^2	2.36×10^{-23}	7.88×10^{-24}	4.73×10^{-24}	2.36×10^{-24}	4.00×10^{-25}
α_2^2	2.36×10^{-23}	7.88×10^{-24}	4.73×10^{-24}	2.36×10^{-24}	4.00×10^{-25}

TABLE V: The same as table IV but for $\sqrt{s}=0.5$ TeV.

Luminosity:	$10fb^{-1}$	$30fb^{-1}$	$50fb^{-1}$	$100fb^{-1}$	$230fb^{-1}$
$\mu_{\tau\tau}$	1.81×10^{-4}	1.37×10^{-4}	1.21×10^{-4}	1.02×10^{-4}	8.25×10^{-5}
α_1^2	3.06×10^{-20}	1.02×10^{-20}	6.12×10^{-21}	3.06×10^{-21}	1.33×10^{-21}
α_2^2	3.06×10^{-20}	1.02×10^{-20}	6.12×10^{-21}	3.06×10^{-21}	1.33×10^{-21}

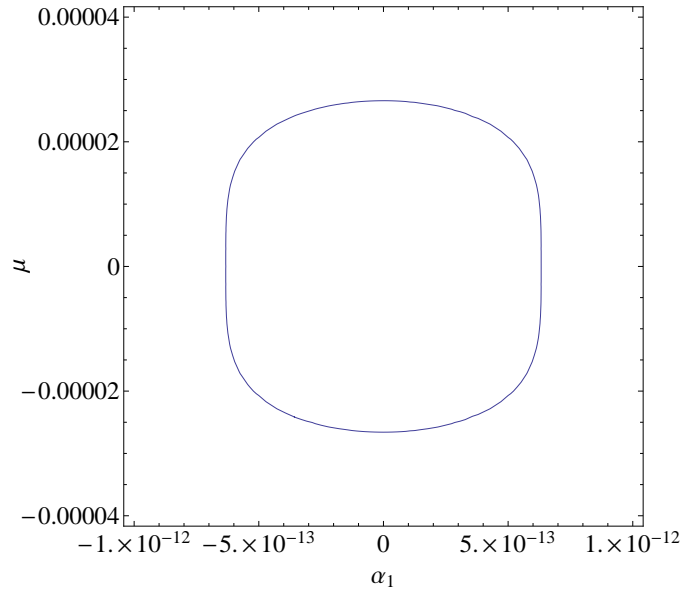


FIG. 10: The contour plot for the upper bounds of the couplings $\mu_{\tau\tau}$ and α_1^2 with 95% C.L. for the process $\gamma\gamma \rightarrow \nu\bar{\nu}$ at $\sqrt{s}=3$ TeV with corresponding design luminosity.

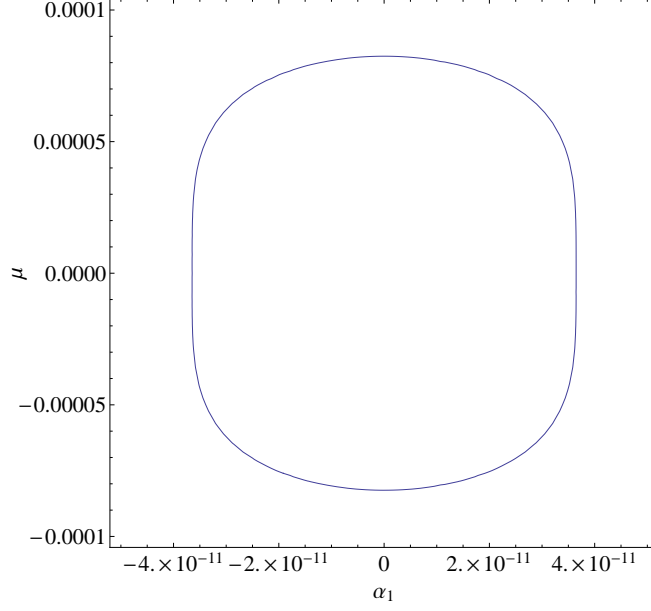


FIG. 11: The same as Fig. 10 but for $\sqrt{s}=0.5$ TeV.

Acknowledgments

We would like to thank I.Sahin for useful comments and discussions. We thanks G. Tavares-Velasco for valuable suggestions about the implementation of $\nu\bar{\nu}\gamma\gamma$ vertex into the CompHEP program.

-
- [1] Y. Fukuda *et al.* [Super-Kamiokande Collaboration], Phys. Rev. Lett. **81**, 1562 (1998).
 - [2] Q. R. Ahmad *et al.* [SNO Collaboration], Phys. Rev. Lett. **89**, 011301 (2002).
 - [3] K. Eguchi *et al.* [KamLAND Collaboration], Phys. Rev. Lett. **90**, 021802 (2003).
 - [4] H. Braun *et al.*, CLIC-NOTE-764, [CLIC Study Team Collaboration], CLIC 2008 parameters, <http://www.clic-study.org>.
 - [5] I. F. Ginzburg, G. L. Kotkin, S. L. Panfil, V. G. Serbo and V. I. Telnov, Nucl. Instrum. Meth. A **219**, 5 (1984).
 - [6] I. F. Ginzburg, G. L. Kotkin, V. G. Serbo and V. I. Telnov, Nucl. Instrum. Meth. **205**, 47 (1983).
 - [7] H. B. Li *et al.* [TEXONO Collaboration], Phys. Rev. Lett. **90**, 131802 (2003) [hep-ex/0212003].
 - [8] Z. Daraktchieva *et al.* [MUNU Collaboration], Phys. Lett. B **615**, 153 (2005) [hep-ex/0502037].

- [9] H. T. Wong *et al.* [TEXONO Collaboration], Phys. Rev. D **75**, 012001 (2007) [hep-ex/0605006].
- [10] H. T. Wong, H. -B. Li and S. -T. Lin, Phys. Rev. Lett. **105**, 061801 (2010) [arXiv:1001.2074 [hep-ph]].
- [11] C. Arpesella *et al.* [The Borexino Collaboration], Phys. Rev. Lett. **101**, 091302 (2008) [arXiv:0805.3843 [astro-ph]].
- [12] G. G. Raffelt, Phys. Rept. **320**, 319 (1999).
- [13] V. Castellani and S. Degl’Innocenti, Astrophys. J. **402**, 574 (1993).
- [14] M. Catelan, J. A. d. Pacheco and J. E. Horvath, Astrophys. J. **461**, 231 (1996) [arXiv:astro-ph/9509062].
- [15] A. Ayala, J. C. D’Olivo and M. Torres, Phys. Rev. D **59**, 111901 (1999) [hep-ph/9804230].
- [16] R. Barbieri and R. N. Mohapatra, Phys. Rev. Lett. **61**, 27 (1988).
- [17] J. M. Lattimer and J. Cooperstein, Phys. Rev. Lett. **61**, 23 (1988).
- [18] A. Heger, A. Friedland, M. Giannotti and V. Cirigliano, Astrophys. J. **696**, 608 (2009) [arXiv:0809.4703 [astro-ph]].
- [19] F. Larios, M. A. Perez and G. Tavares-Velasco, Phys. Lett. B **531**, 231 (2002) [hep-ph/0201024].
- [20] A. Pukhov *et al.*, arXiv:hep-ph/9908288.
- [21] I. Sahin, Phys. Rev. D **85**, 033002 (2012) [arXiv:1201.4364 [hep-ph]].
- [22] I. Sahin and M. Koksul, JHEP **1103**, 100 (2011) [arXiv:1010.3434 [hep-ph]].
- [23] R. Schwienhorst *et al.* [DONUT Collaboration], Phys. Lett. B **513**, 23 (2001) [arXiv:hep-ex/0102026].
- [24] S. Davidson, M. Gorbahn and A. Santamaria, Phys. Lett. B **626**, 151 (2005) [arXiv:hep-ph/0506085].